IAI Journals.ASM.org

Evaluation of the Immunogenicity and Vaccine Potential of Recombinant *Plasmodium falciparum* Merozoite Surface Protein 8

James R. Alaro,[a] Evelina Angov,[b] Ana M. Lopez,[a] Hong Zhou,[c] Carole A. Long,[a,c] and James M. Burns, Jr.[a]

Center for Molecular Parasitology, Department of Microbiology and Immunology, Drexel University College of Medicine, Philadelphia, Pennsylvania, USA[a]; U.S. Military Malaria Research Program, Malaria Vaccine Branch, Walter Reed Army Institute of Research, Silver Spring, Maryland, USA[b]; and Malaria Immunology Section, Laboratory of Malaria and Vector Research, National Institute of Allergy and Infectious Diseases, National Institutes of Health, Rockville, Maryland, USA[c]

The C-terminal 19-kDa domain of merozoite surface protein 1 ($MSP1_{19}$) is the target of protective antibodies but alone is poorly immunogenic. Previously, using the *Plasmodium yoelii* murine model, we fused *P. yoelii* $MSP1_{19}$ (*Py*$MSP1_{19}$) with full-length *P. yoelii* merozoite surface protein 8 (MSP8). Upon immunization, the MSP8-restricted T cell response provided help for the production of high and sustained levels of protective *Py*$MSP1_{19}$- and *Py*MSP8-specific antibodies. Here, we assessed the vaccine potential of MSP8 of the human malaria parasite, *Plasmodium falciparum*. Distinct from *Py*MSP8, *P. falciparum* MSP8 (*Pf*MSP8) contains an N-terminal asparagine and aspartic acid (Asn/Asp)-rich domain whose function is unknown. Comparative analysis of recombinant full-length *Pf*MSP8 and a truncated version devoid of the Asn/Asp-rich domain, *Pf*MSP8(ΔAsn/Asp), showed that both proteins were immunogenic for T cells and B cells. All T cell epitopes utilized mapped within r*Pf*MSP8(ΔAsn/Asp). The dominant B cell epitopes were conformational and common to both r*Pf*MSP8 and r*Pf*MSP8(ΔAsn/Asp). Analysis of native *Pf*MSP8 expression revealed that *Pf*MSP8 is present intracellularly in late schizonts and merozoites. Following invasion, *Pf*MSP8 is found distributed on the surface of ring- and trophozoite-stage parasites. Consistent with a low and/or transient expression of *Pf*MSP8 on the surface of merozoites, *Pf*MSP8-specific rabbit IgG did not inhibit the *in vitro* growth of *P. falciparum* blood-stage parasites. These studies suggest that the further development of *Pf*MSP8 as a malaria vaccine component should focus on the use of *Pf*MSP8(ΔAsn/Asp) and its conserved, immunogenic T cell epitopes as a fusion partner for protective domains of poor immunogens, including *Pf*$MSP1_{19}$.

Plasmodium falciparum remains the leading cause of malaria morbidity and mortality (24). Achieving the goal of eradicating *P. falciparum* malaria worldwide will almost certainly require the development of an efficacious vaccine that includes a blood-stage component. One intensively investigated blood-stage malaria vaccine candidate is merozoite surface protein 1 (MSP1). MSP1 is an essential and abundant surface protein expressed during schizogony as an ~200-kDa precursor protein (30). Prior to the schizont rupture, MSP1 is proteolytically processed to produce the 83-, 30-, 38-, and 42-kDa fragments (31, 36, 38) that remain noncovalently associated along with MSP6, MSP7, and MSP9 (34, 44, 53) and tethered to the surface by the glycosylphosphatidylinositol (GPI)-anchored 42-kDa fragment ($MSP1_{42}$) (43, 44). During invasion, $MSP1_{42}$ is further cleaved into $MSP1_{33}$ and $MSP1_{19}$ (25, 26) to release the entire complex except for $MSP1_{19}$ that remains GPI anchored and is carried into the newly invaded red blood cell (RBC) (7, 19). $MSP1_{19}$ consists almost entirely of two conserved epidermal growth factor (EGF)-like domains (30).

$MSP1_{19}$ is well established as a critical target of merozoite-neutralizing, protective antibodies (7, 11, 12, 16, 23, 29, 33, 35, 41). Upon immunization with $MSP1_{19}$, however, T cell recognition of $MSP1_{19}$ is weak and limits the $CD4^+$ T cell-dependent production of $MSP1_{19}$-specific antibodies by B cells (22, 27, 50). Indeed, vaccine-induced protection in experimental models has almost always required fusion of $MSP1_{19}$ to heterologous T cell epitopes and/or formulation with Freund's adjuvant. This approach, however, is limited by the fact that heterologous T cell responses cannot be boosted by natural infection and that Freund's adjuvant is toxic for human use. Unfortunately, immunization of human subjects with the larger *P. falciparum* $MSP1_{42}$ (*Pf*$MSP1_{42}$) vaccine also did not solve the problem, as protective levels of $MSP1_{19}$-specific antibodies were not elicited (42). In an alternative approach to improve immunogenicity and efficacy of MSP1-based vaccines, we identified merozoite surface protein 8 (MSP8) as a potential fusion partner for $MSP1_{19}$.

MSP8 was originally identified in *P. yoelii* as a 46-kDa protein with an N-terminal signal sequence, a C-terminal GPI anchor, and two C-terminal EGF-like domains with significant homology to the protective EGF-like domains of $MSP1_{19}$ (10). Immunization with full-length recombinant *Py*MSP8 (r*Py*MSP8) alone confers antibody-dependent protection against lethal *P. yoelii* 17XL malaria (10, 48). In subsequent studies, we showed that by coupling *Py*$MSP1_{19}$ to full-length *Py*MSP8, the immunogenicity of *Py*$MSP1_{19}$ was markedly improved, with the chimeric *Py*MSP1/8 vaccine affording superior protection compared to immunization with r*Py*$MSP1_{42}$ and r*Py*MSP8, alone or in combination (49). Importantly, the *Py*MSP8-restricted T cell response elicited by the chimeric *Py*MSP1/8 vaccine was sufficient to provide the help for *Py*$MSP1_{19}$-specific B cells to produce high and sustained levels of protective antibodies (1). These data provide strong support for the further development of a *P. falciparum* $MSP1_{19}$ and MSP8 vaccine.

Received 27 February 2012 **Returned for modification** 19 March 2012
Accepted 1 May 2012
Published ahead of print 14 May 2012
Editor: J. H. Adams
Address correspondence to James M. Burns, Jr., jburns@drexelmed.edu.
Supplemental material for this article may be found at http://iai.asm.org/.

doi:10.1128/IAI.00211-12

While much is known about *Pf*MSP1$_{19}$, the vaccine potential of *P. falciparum* MSP8 has not been adequately evaluated. Comparative analysis of *P. falciparum* and *P. yoelii* MSP8 sequences reveals an overall sequence identity of ~33% and similarity of ~56% with a high conservation of their double EGF-like domains (47% identity, 67% similarity). Distinctively, *Pf*MSP8 contains an asparagine and aspartic acid (Asn/Asp)-rich domain of ~170 amino acids near the N terminus that is absent in MSP8 of *P. yoelii*, *Plasmodium berghei*, *Plasmodium chabaudi*, *Plasmodium knowlesi*, and *Plasmodium vivax*. Among different *P. falciparum* isolates, MSP8 is highly conserved, exhibiting 95% amino acid identity with slight variations limited to small insertions or deletions in the Asn/Asp-rich domain (5). Remarkably, the remaining C-terminal sequence, including the double EGF-like domains, is invariant. Previously, it was reported that *Pf*MSP8 is transcribed and translated in ring-stage parasites and may be involved in the formation/function of the parasitophorous vacuolar membrane (5, 6, 21). This is unusual given that many of the MSPs implicated in the invasion process are expressed in maturing schizonts (9). Nevertheless, the EGF-like domains of *Pf*MSP1 can be replaced with those of *P. berghei* MSP8 with no apparent effect on the *in vitro* growth of the transgenic *P. falciparum* parasites (20).

Based on limited studies, it appears that *Pf*MSP8 is naturally immunogenic during infection in humans. Curiously though, sera from malaria-exposed adults appear to recognize B cell epitopes within the first 350 amino acids of *Pf*MSP8 that contain the Asn/Asp-rich domain but only weakly recognize those associated with the C-terminal EGF-like domains (5, 21). While the contribution of *Pf*MSP8-specific antibodies to natural immunity has not been investigated, the potential involvement of antibodies to the Asn/Asp-rich domain is of interest. Thus far, there are no reports evaluating the ability of *Pf*MSP8-specific antibodies to inhibit the *in vitro* growth of *P. falciparum* blood-stage parasites. The present study focuses on the evaluation of the vaccine potential of r*Pf*MSP8 with or without the Asn/Asp-rich domain considering (i) the specificity of immunization-induced T and B cell responses, (ii) the expression, processing, and localization of native *Pf*MSP8, and (iii) the ability of *Pf*MSP8-specific antibodies to inhibit the *in vitro* growth of *P. falciparum*. Similarities and differences in MSP8 between *P. falciparum* and *P. yoelii* are discussed.

MATERIALS AND METHODS

r*Pf*MSP8 and r*Pf*MSP8(ΔAsn/Asp) expression constructs. The complete coding sequence of *P. falciparum* MSP8 (FVO strain; GenBank accession no. AF325161.1) was subjected to codon harmonization (see Fig. S1 in the supplemental material) using previously described algorithms for expression in *Escherichia coli* (4). Codon harmonization, believed to promote proper folding of protein subdomains (52), has been used successfully to produce r*Pf*MSP1$_{42}$ (FVO) (3), r*Pf*LSA1 (28), and r*Pf*s48/45 (13) vaccines. The coding sequence of the full-length recombinant protein, r*Pf*MSP8, was based on amino acids 27 to 577, excluding the N-terminal signal sequence and the C-terminal hydrophobic anchor sequence, both predicted to be cleaved off the mature protein. The truncated form, r*Pf*MSP8(ΔAsn/Asp), was based on amino acids 221 to 577 devoid of the N-terminal Asp/Asn-rich domain. A leader sequence that includes a 6-histidine tag and a glycine-serine linker (MAHHHHHHPGGSGSGT) was inserted onto the 5′ end of both codon-harmonized coding sequences to allow for downstream purification. Two stop codons (TGA and TAA) were incorporated at the 3′ end of each sequence. To facilitate subcloning, NcoI and NotI restriction sites were added to the 5′ and 3′ ends, respectively. The codon-harmonized r*Pf*MSP8 and r*Pf*MSP8(ΔAsn/Asp) constructs were commercially synthesized, cloned into pBR322 and pUCminusMCS cloning vectors, respectively, and sequenced (Blue Heron Biotechnology Inc., Bothell, WA). The synthetic gene inserts were excised and ligated into the NcoI and NotI sites of the pET-28 expression vector (EMD Biosciences, San Diego, CA). The resulting expression vectors were transformed into SHuffle T7 Express *lysY*-competent *E. coli* cells (New England BioLabs, Ipswich, MA). This strain (i) is devoid of glutaredoxin reductase and thioredoxin reductase genes (Δ*gor* Δ*trxB*) allowing for disulfide bond formation and (ii) expresses a cytoplasmic disulfide bond isomerase (DsbC) that promotes proper folding in the cytoplasm (17).

Expression of the recombinant proteins was accomplished using a BioFLo115 benchtop bioreactor (New Brunswick Scientific, Edison, NJ). Three liters of defined medium containing 36 g/liter Bacto tryptone (Becton Dickinson, San Jose, CA), 12 g/liter Bacto yeast extract (Becton Dickinson), 16.43 g/liter K_2HPO_4, 2.31 g/liter KH_2PO_4, 4 ml/liter glycerol (Sigma-Aldrich, St. Louis, MO), and 30 mg/liter kanamycin (Invitrogen, Carlsbad, CA) was inoculated with 150 ml of starter culture grown in selective LB medium overnight at 30°C in a shaking incubator. The bioreactor temperature was maintained at 30°C, and dissolved oxygen was maintained at 30% saturation by a combination of a cascade agitation set between 200 and 600 rpm and an airflow rate of 5 liters per minute. The pH was continuously monitored and maintained at 7.2. Foaming was suppressed by controlled supply of antifoam B (Sigma-Aldrich). At a cell density for which the optical density at 600 nm (OD_{600}) was approximately 4, expression was induced by the addition of isopropyl β-D-1-thiogalactopyranoside (IPTG; Fisher Scientific, Pittsburg, PA) to a final concentration of 1 mM. Three hours postinduction, cells were harvested by centrifugation at 8,000 × *g* for 20 min at 4°C, and cell pastes were stored frozen at −80°C.

Purification of r*Pf*MSP8 and r*Pf*MSP8(ΔAsn/Asp). The purification protocol was the same for both r*Pf*MSP8 and r*Pf*MSP8(ΔAsn/Asp). The cell paste was resuspended in 5 ml/g of BugBuster HT protein extraction reagent (EMD Biosciences) in the presence of 25 units/ml of benzonase nuclease (EMD Biosciences) and 1 KU/ml of recombinant lysozyme (EMD Biosciences) and mixed for 30 min at room temperature. The lysate was clarified by centrifugation at 20,000 × *g* for 15 min. The resulting pellet was resuspended in half the volume of BugBuster reagent used in the initial lysis plus an additional 1 KU/ml of recombinant lysozyme, rocked for 10 min, and centrifuged at 5,800 × *g* for 15 min. The final pellet was resuspended in 5 ml/g (starting material) of binding buffer (20 mM Tris-HCl [pH 7.9], 5 mM imidazole, 0.5 M NaCl) containing 0.2% *N*-lauroylsarcosine sodium salt (Sarkosyl; Sigma-Aldrich) and incubated overnight at 4°C with mixing. Both r*Pf*MSP8 and r*Pf*MSP8(ΔAsn/Asp) were completely solubilized with residual insoluble material removed by centrifugation at 20,000 × *g* for 10 min. The detergent-soluble fractions were purified by nickel-chelate affinity chromatography under nondenaturing conditions as previously described (49). The eluted r*Pf*MSP8 and r*Pf*MSP8(ΔAsn/Asp) were dialyzed overnight at 4°C against 4 liters of binding buffer containing 0.2% sarkosyl. The final protein concentration was determined by bicinchoninic acid protein assay (BCA; Thermo Scientific, Rockford, IL). Protein purity and conformation were assessed by Coomassie blue staining following SDS-PAGE on 10% gels, run under both reduced and nonreduced conditions. Corresponding immunoblots were probed with an anti-His tag monoclonal antibody (EMD Biosciences). Reduced and alkylated (R/A) r*Pf*MSP8 and r*Pf*MSP8(ΔAsn/Asp) were prepared by sequential treatment with dithiothreitol (Sigma-Aldrich) and iodoacetic acid (Thermo Scientific) as previously described (48).

Production of rabbit antiserum and purification of IgG. Polyclonal rabbit antisera and IgG fractions were generated by Lampire Biological Laboratories (Pipersville, PA) following their classic-line basic protocol. Briefly, rabbits were immunized once with 200 μg of either r*Pf*MSP8 or r*Pf*MSP8(ΔAsn/Asp) formulated with complete Freund's adjuvant (CFA) followed by 4 booster immunizations (200 μg each) with the same antigen formulated in incomplete Freund's adjuvant (IFA). A control rabbit was

immunized as described above with CFA/IFA alone. Approximately 2 weeks after the final immunization, antisera were recovered. The IgG fraction of each antiserum was purified by protein A affinity chromatography and dialyzed into 0.01 M sodium phosphate, 0.15 M NaCl [pH 7.4].

Direct-binding and competitive ELISAs. The antigen-specific antibody responses induced by immunization with r*Pf*MSP8 or r*Pf*MSP8(ΔAsn/Asp) were measured by direct-binding enzyme-linked immunosorbent assay (ELISA) as previously described (1). Briefly, ELISA plates coated with 0.25 μg per well of purified r*Pf*MSP8 or r*Pf*MSP8 (ΔAsn/Asp) were incubated with 2-fold serial dilutions of mouse or rabbit sera starting at 1:10,000 or purified rabbit IgG starting at 2 μg/ml. Corresponding adjuvant control sera or IgG were used as negative controls. Bound antibodies were detected by horseradish peroxidase-conjugated rabbit anti-mouse IgG (Thermo Scientific) or goat anti-rabbit IgG (Invitrogen) with ABTS [2,2′-azinobis(3-ethylbenzthiazolinesulfonic acid)] as the substrate. A_{405} values of between 1.0 and 0.1 were plotted, and titers were calculated as the reciprocal of the dilution that yielded an A_{405} of 0.5.

For the competitive ELISAs, an initial titration was performed to determine an IgG concentration that resulted in an OD of ~1.0 as the optimal dilution in the assay. Anti-r*Pf*MSP8 IgG or anti-r*Pf*MSP8(ΔAsn/Asp) IgG at a constant concentration of 5 ng/ml was preincubated overnight at 4°C with increasing concentrations (0, 0.1, 1, 10, 100, 1,000, and 10,000 ng/ml) of r*Pf*MSP8, R/A r*Pf*MSP8, r*Pf*MSP8(ΔAsn/Asp), or R/A r*Pf*MSP8(ΔAsn/Asp) as indicated in buffer containing 20 mM Tris-HCl (pH 8.0), 50 mM NaCl, 5 mM EDTA, 0.5% Triton X-100, and 0.5% deoxycholate. Residual binding of the test IgG to plate-bound recombinant antigen was then determined by ELISA as described above. The percent residual binding of test IgG after incubation with various concentrations of inhibitors was calculated as (OD of IgG in the presence of inhibitor/OD of IgG without inhibitor) × 100. The molar concentration of inhibitor resulting in 50% inhibition of IgG binding (IC_{50}) was calculated using GraphPad Prism (La Jolla, CA).

Comparative immunogenicity of r*Pf*MSP8 and r*Pf*MSP8(ΔAsn/Asp) in mice. Male CB6F1/J (BALB/cJ × C57BL/6J) mice, 5 to 6 weeks of age, were purchased from The Jackson Laboratory and housed in the Animal Care Facility of Drexel University College of Medicine under specific pathogen-free conditions. Groups of CB6F1/J mice ($n = 5$) were immunized subcutaneously with 10 μg/dose of purified r*Pf*MSP8 or r*Pf*MSP8(ΔAsn/Asp) formulated with either (i) 25 μg/dose of Quil A as the adjuvant (Accurate Chemical and Scientific Corporation, Westbury, NY) or (ii) 10 μg/dose of CpG oligodeoxynucleotide (ODN) 1826 (Eurofins MWG Operon, Huntsville, AL) and emulsified in Montanide ISA 720 VG (Seppic Inc., Paris, France) at a ratio of 70:30 (vol/vol). Control mice were immunized with the corresponding adjuvants alone. All mice were boosted twice at 3-week intervals with the same antigen/adjuvant formulation used in the priming immunization. For antibody assays, sera were collected 2 weeks after the third immunization and stored at −80°C until use. For T cell assays, mice were rested for approximately 10 weeks and then boosted intraperitoneally with 10 μg/dose of r*Pf*MSP8 or r*Pf*MSP8(ΔAsn/Asp) formulated with Quil A or CpG ODN. Control mice received adjuvant alone. Two weeks later, spleens were harvested and processed for T cell proliferation assays as previously described (1).

T cell proliferation assay. Sixty 18-mer peptides (see Table S1 in the supplemental material) spanning the entire length of *Pf*MSP8 FVO (excluding the N-terminal signal and C-terminal anchor sequences) were custom synthesized and purified (GenScript USA Inc., Piscataway, NJ). These peptides overlapped by 9 amino acids and were >90% pure. The lyophilized peptides were reconstituted to a working concentration of 1 mg/ml as recommended by the manufacturer. T cell proliferation induced by the recombinant antigens or peptides was measured as previously described (1). Briefly, 1×10^5 splenocytes per well were plated in triplicate in 96-well round-bottom plates (Becton Dickinson) and stimulated with 5 μg/ml of r*Pf*MSP8 or r*Pf*MSP8(ΔAsn/Asp) or with 15 μg/ml of individual peptides for 4 days and pulsed with 1 μCi per well of methyl [^{3}H]thymidine (40 to 60 Ci/mmol; GE Healthcare, Piscataway, NJ) for the last 18 h of incubation. An additional set of cells was stimulated with 1 μg/ml of concanavalin A (Sigma-Aldrich) or left unstimulated to serve as positive or negative controls, respectively. The stimulation index was calculated as the mean counts per minute of stimulated wells divided by the mean counts per minute of unstimulated wells.

***P. falciparum* cultures and stage-specific antigen preparations.** *P. falciparum* FVO strain (ATCC, Manassas, VA) parasites were maintained *in vitro* in complete medium (RPMI 1640 medium [Sigma-Aldrich] supplemented with 2 mM L-glutamine, 10 μg/ml hypoxanthine, 20 mM HEPES [pH 7.4], 25 mM $NaHCO_3$, 20 mM glucose, 1× streptomycin-penicillin, and 0.25% Albumax II [Invitrogen]) at 4% hematocrit of O+ human RBCs (Interstate Blood Bank, Inc., Memphis, TN) in 90% N_2, 5% CO_2, and 5% O_2 (45). Parasites were tightly synchronized by a series of treatments with 5% D-sorbitol (Sigma-Aldrich), and parallel cultures were harvested at 2, 8, 14, 20, 26, 32, 40, and 48 h of the asexual cycle. RBCs were lysed by treatment with 0.15% saponin in phosphate-buffered saline (PBS) for 10 min, and intact parasites were pelleted by centrifugation, washed, and stored at −80°C until use. To isolate free merozoites, synchronized late-stage parasites (40 to 42 h) were treated with the protease inhibitor, *trans*-epoxysuccinyl-L-leucylamido-(4-guanidino)butane (E64; Sigma-Aldrich), at a concentration of 10 μM for 6 h. Fully mature, segmented schizonts were recovered by centrifugation, and merozoites were mechanically released by passage through a 1.2-μm Acrodisc 32-mm syringe filter (Pall Corporation, Port Washington, NY) (8). Free merozoites were recovered by high-speed centrifugation at 10,000 rpm for 10 min, and pellets were stored frozen at −80°C. Cytosolic and membrane fractions of parasite proteins were prepared by two cycles of temperature-dependent separation of aqueous and detergent phases of parasites solubilized in 5% Triton X-114 (Thermo Scientific) as previously described (10, 51).

Indirect immunofluorescence assay. Indirect immunofluorescence assays were conducted as previously described using acetone-methanol-fixed RBCs infected with asynchronously grown *P. falciparum* FVO (47). Fixed cells were costained with 1 μg/ml of either rabbit anti-r*Pf*MSP8 IgG or rabbit anti-r*Pf*MSP8(ΔAsn/Asp) IgG and monoclonal antibody (MAb) 5.2 (mouse anti-*Pf*MSP1$_{19}$ FVO; ATCC-MR4) or MAb 4G2 (rat anti-*Pf*AMA1 FVO) (14). Negative controls were stained with 1 μg/ml rabbit adjuvant control IgG and 1:500 normal mouse serum. Bound IgG was detected with tetramethylrhodamine (TRITC)-conjugated goat anti-rabbit IgG (Invitrogen) and fluorescein isothiocyanate (FITC)-conjugated goat anti-mouse IgG (Invitrogen) (1:400). Slides were then mounted with SlowFade Gold antifade reagent with DAPI (4′,6-diamidino-2-phenylindole) (Invitrogen), and images were acquired using an Olympus BX60 fluorescence microscope (Olympus America Inc., Melville, NY) and a SPOT RT slider digital camera system (Diagnostic Instruments, Sterling Heights, MI). Secondary antibodies for colocalization studies of *Pf*MSP8 and *Pf*MSP1 or *Pf*AMA1 in free merozoites by confocal microscopy utilized Alexa Fluor 488-conjugated goat anti-mouse or rat IgG and Alexa Fluor 568-conjugated goat anti-rabbit IgG (1:500; Invitrogen). Images were generated using a Leica SP2 confocal microscope (Leica Microsystems, Buffalo Grove, IL) and visualized using Bitplane Imaris software (Bitplane Inc., South Windsor, CT).

***P. falciparum* growth inhibition assays.** The growth inhibitory activity (GIA) of the purified rabbit anti-r*Pf*MSP8, anti-r*Pf*MSP8(ΔAsn/Asp), or adjuvant control IgG toward *P. falciparum* (FVO) was assessed *in vitro* by the measurement of parasite lactate dehydrogenase activity (39) or [^{3}H]hypoxanthine incorporation (18, 45) using standard protocols. Each rabbit IgG was tested at final concentrations ranging between 0.5 mg/ml and 5 mg/ml as indicated. Growth inhibitory activity was calculated relative to *P. falciparum* blood-stage parasites growing in complete medium in the absence of any added rabbit IgG.

Statistical analysis. The statistical significance of the differences in antigen-specific IgG titers and T cell proliferation stimulation indices was determined by two-tailed, unpaired Student's *t* test, with probability (*P*) values of <0.05 considered significant.

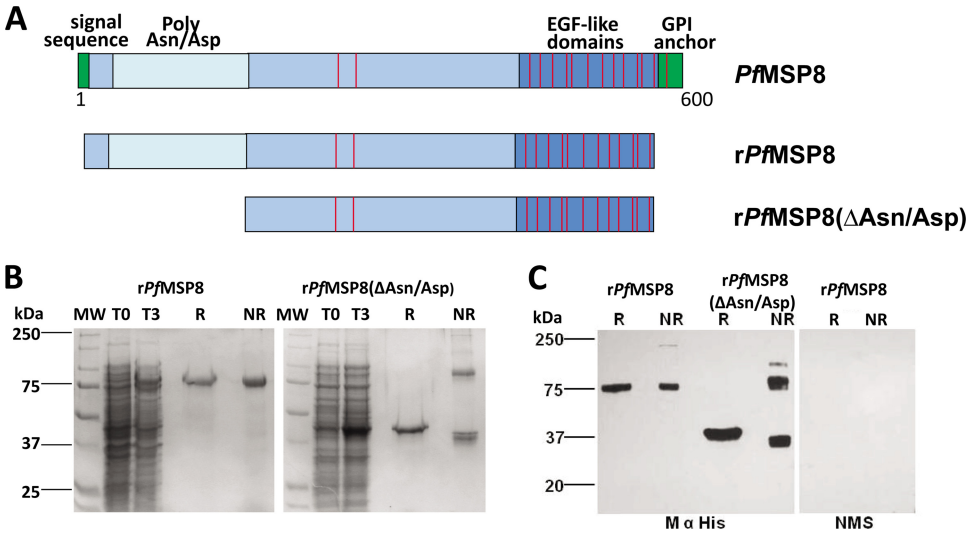

FIG 1 Expression and purification of r*Pf*MSP8 and r*Pf*MSP8(ΔAsn/Asp). (A) Schematic depiction of the amino acid sequences of r*Pf*MSP8 (567 residues) and r*Pf*MSP8(ΔAsn/Asp) (373 residues) in relation to the native sequence of *P. falciparum* (FVO) MSP8. Positions of the conserved cysteine residues are indicated by the red lines. (B) Coomassie blue-stained 10% SDS-polyacrylamide gel containing lysates of *E. coli* (reduced) expressing the r*Pf*MSP8 and r*Pf*MSP8(ΔAsn/Asp) at the time of induction (T0) or 3 h postinduction (T3) and nickel-chelate affinity-purified proteins (3 μg per lane) under reducing (R) and nonreducing (NR) conditions. (C) Immunoblot analysis of the purified proteins (0.1 μg per lane) under reducing (R) and nonreducing (NR) conditions probed with anti-His tag monoclonal antibody. Normal mouse serum (NMS) served as a negative control. Molecular weight markers in kilodaltons (kDa) are indicated.

RESULTS

Codon harmonization, expression, and purification of r*Pf*MSP8 and r*Pf*MSP8(ΔAsn/Asp). Initial attempts to produce full-length r*Pf*MSP8 in bacteria using constructs based on the native gene sequence of *Pf*MSP8 failed completely. Two expression vectors encoding the full-length r*Pf*MSP8 and the truncated r*Pf*MSP8 (ΔAsn/Asp) were then constructed based on the *E. coli* codon-harmonized gene sequence of *Pf*MSP8 (FVO) (see Fig. S1 in the supplemental material), as diagramed in Fig. 1A. A pET/T7 RNA polymerase expression system, with the pET-28 plasmid and SHuffle T7 Express *lysY E. coli* cells as the host, was used for production. The r*Pf*MSP8 and r*Pf*MSP8(ΔAsn/Asp) proteins were successfully purified under nondenaturing conditions by nickel-chelate affinity chromatography with final yields of 2 mg/g wet cells and 3 mg/g wet cells, respectively. The integrity and purity of the purified recombinant proteins was assessed by SDS-PAGE. Purified r*Pf*MSP8 migrated as a single band of ~75 kDa under reducing conditions and exhibited a slightly faster mobility under nonreducing conditions with no higher molecular weight aggregates observed (Fig. 1B). Purified r*Pf*MSP8(ΔAsn/Asp) migrated as a single band of ~46 kDa under reducing conditions (Fig. 1B). Under nonreducing conditions, two r*Pf*MSP8(ΔAsn/Asp) bands were observed; a faster-migrating band of ~40 kDa and a second higher-molecular-weight band of ~80 kDa (Fig. 1B). Reduced and alkylated preparations of r*Pf*MSP8 and r*Pf*MSP8(ΔAsn/Asp) migrated as single bands under both reducing and nonreducing conditions (data not shown). The corresponding immunoblots probed with an anti-His tag monoclonal antibody revealed similar patterns of migration for both r*Pf*MSP8 and r*Pf*MSP8(ΔAsn/Asp) (Fig. 1C). The reduction-sensitive mobility shifts and the lack of large-molecular-weight aggregates exhibited by both recombinant proteins on SDS-PAGE suggest that disulfide bonds formed correctly. In the absence of the Asn/Asp-rich domain, a single interchain disulfide bond formed in r*Pf*MSP8(ΔAsn/Asp), resulting in a 1:1 mix of monomers and dimers in the final product.

r*Pf*MSP8 and r*Pf*MSP8(ΔAsn/Asp) share conformation-dependent, immunodominant B cell epitopes. To evaluate similarity in conformational and linear B cell epitopes of r*Pf*MSP8 and r*Pf*MSP8(ΔAsn/Asp) and determine if the Asn/Asp-rich domain is a significant target of antibody responses, high-titer polyclonal rabbit antisera were raised by immunization with r*Pf*MSP8 and r*Pf*MSP8(ΔAsn/Asp). As measured by ELISA (Fig. 2A), immunization with r*Pf*MSP8 induced a strong antibody response with titers of 328,821 and 276,316 when measured against r*Pf*MSP8 and r*Pf*MSP8(ΔAsn/Asp), respectively. Likewise, immunization with r*Pf*MSP8(ΔAsn/Asp) elicited an equally strong antibody response with titers of 410,610 and 373,733 when measured against r*Pf*MSP8 and r*Pf*MSP8(ΔAsn/Asp), respectively. Data from this initial assessment indicate that the immunogenicities of r*Pf*MSP8 and r*Pf*MSP8(ΔAsn/Asp) are comparable and suggested that B cell epitopes common to both antigens are dominant.

To evaluate the nature and similarity of B cell epitopes associated with r*Pf*MSP8 and r*Pf*MSP8(ΔAsn/Asp) in greater detail, purified IgG from rabbit anti-r*Pf*MSP8 and anti-r*Pf*MSP8(ΔAsn/Asp) sera were analyzed in competitive ELISAs. In the first set of assays, the capacity of r*Pf*MSP8, R/A r*Pf*MSP8, or r*Pf*MSP8(ΔAsn/Asp) to inhibit the binding of anti-r*Pf*MSP8 IgG to plate-bound r*Pf*MSP8 was tested. As shown in Fig. 2B, r*Pf*MSP8 efficiently inhibited the binding of anti-r*Pf*MSP8 IgG (IC_{50} = 57 pM), with 100% inhibition achieved with higher antigen concentrations. In contrast, R/A r*Pf*MSP8, with its disulfide-dependent determinants disrupted, only marginally inhibited the binding of anti-r*Pf*MSP8 IgG (IC_{50} > 10 nM). Of particular interest, r*Pf*MSP8 (ΔAsn/Asp) was also a potent inhibitor of the binding of anti-r*Pf*MSP8 IgG to r*Pf*MSP8-coated plates with an IC_{50} of 18 pM, similar to that described above with full-length r*Pf*MSP8 as the competitor. However, r*Pf*MSP8(ΔAsn/Asp) could not inhibit ~20% of the binding of anti-r*Pf*MSP8 IgG to r*Pf*MSP8 regardless of the amount of the inhibitor added. These data show that the majority of the anti-r*Pf*MSP8 antibodies are directed toward con-

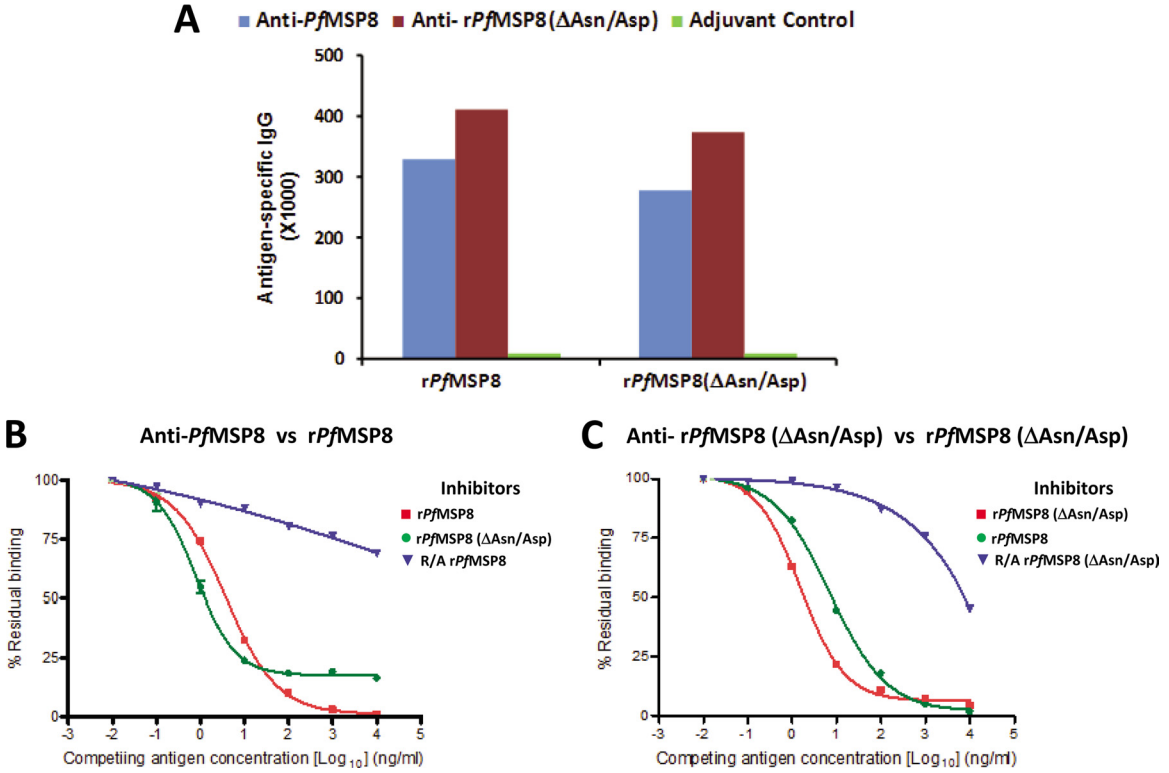

FIG 2 Deletion of the Asn/Asp-rich domain does not alter the conformational integrity or B cell immunogenicity of r*Pf*MSP8. (A) Antigen-specific IgG titers in sera of rabbits immunized with r*Pf*MSP8 (blue), r*Pf*MSP8(ΔAsn/Asp) (red), or adjuvants alone (green) were compared by direct-binding ELISA on plates coated with homologous or heterologous antigens as indicated on the *x* axis. For competitive ELISAs, a constant concentration of 5 ng/ml of anti-r*Pf*MSP8 (B) or anti-r*Pf*MSP8(ΔAsn/Asp) (C) IgG was preincubated with increasing concentrations of intact homologous antigen (■), intact heterologous antigen (●), or R/A homologous antigen (▼), and residual binding to plate-bound homologous antigen was determined by ELISA. The percent residual binding at various competing antigen (inhibitor) concentrations was calculated as (OD of IgG in the presence of inhibitor/OD of same IgG without inhibitor) × 100.

formation-dependent epitopes common to both r*Pf*MSP8 and r*Pf*MSP8(ΔAsn/Asp). A measurable but small proportion of r*Pf*MSP8-induced antibodies recognize epitopes contained within the N-terminal Asn/Asp-rich domain.

In the second set of assays, the capacity of r*Pf*MSP8, r*Pf*MSP8(ΔAsn/Asp), or R/A r*Pf*MSP8(ΔAsn/Asp) to inhibit binding of anti-r*Pf*MSP8(ΔAsn/Asp) IgG to plate-bound r*Pf*MSP8 (ΔAsn/Asp) was tested. As shown in Fig. 2C, r*Pf*MSP8(ΔAsn/Asp) and full-length r*Pf*MSP8 exhibited near-complete inhibition of anti-r*Pf*MSP8(ΔAsn/Asp) IgG binding with similar IC_{50} values of 35 pM and 104 pM, respectively. Conversely, R/A r*Pf*MSP8(ΔAsn/Asp) was a poor inhibitor of anti-r*Pf*MSP8(ΔAsn/Asp) IgG binding ($IC_{50} > 1{,}000$ pM). These data confirm that the overall conformation of the domain common to r*Pf*MSP8 and r*Pf*MSP8 (ΔAsn/Asp) is quite similar between the two antigens and that this domain contains immunodominant, disulfide-dependent B cell epitopes.

Immunization with r*Pf*MSP8 and r*Pf*MSP8(ΔAsn/Asp) elicits robust B cell and T cell responses in mice. To further characterize the immunogenicity of r*Pf*MSP8 and r*Pf*MSP8(ΔAsn/Asp) for B cells and T cells, CB6F1/J mice were immunized with the respective antigens formulated with either Quil A or Montanide and CpG as the adjuvant. The titer of antigen-specific antibodies induced by each formulation was measured by ELISA. As shown in Fig. 3A and B, immunization with r*Pf*MSP8 or r*Pf*MSP8(ΔAsn/Asp) elicited high, comparable, and cross-reactive antibody responses with no significant differences noted between the two antigens ($P > 0.1$). With both r*Pf*MSP8 and r*Pf*MSP8(ΔAsn/Asp), formulations with Quil A were more effective than those with Montanide and CpG as the adjuvant with ~2-fold-higher IgG titers ($P < 0.01$). To assess immunogenicity for T cells, splenocytes from each group of mice were stimulated *in vitro* with either r*Pf*MSP8 or r*Pf*MSP8(ΔAsn/Asp), and the proliferative responses were compared. Regardless of the immunogen, both r*Pf*MSP8 and r*Pf*MSP8(ΔAsn/Asp) induced high and comparable proliferation of splenocytes relative to adjuvant controls (Fig. 3C and D). However, the level of proliferation was also dependent on the adjuvant platform used, with splenocytes from the Quil A groups showing higher responses than the Montanide and CpG groups ($P < 0.01$). A low-level, nonspecific T cell response to r*Pf*MSP8 was consistently noted in control mice irrespective of the adjuvant used (Fig. 3C and D).

Deletion of the Asn/Asp-rich domain of r*Pf*MSP8 does not alter T cell epitope usage. To assess recognition of the Asn/Asp-rich domain of *Pf*MSP8 and determine if deletion of this domain altered antigen processing and T cell epitope usage, splenocytes from r*Pf*MSP8- or r*Pf*MSP8(ΔAsn/Asp)-immunized mice were stimulated with overlapping synthetic peptides covering the entire length of r*Pf*MSP8. As shown in Fig. 4A, five peptides (26, 47, 48, 50, 54) consistently induced significant proliferation of T cells from r*Pf*MSP8 and Quil A-immunized mice. All five peptides mapped within the coding sequence of r*Pf*MSP8(ΔAsn/Asp), with

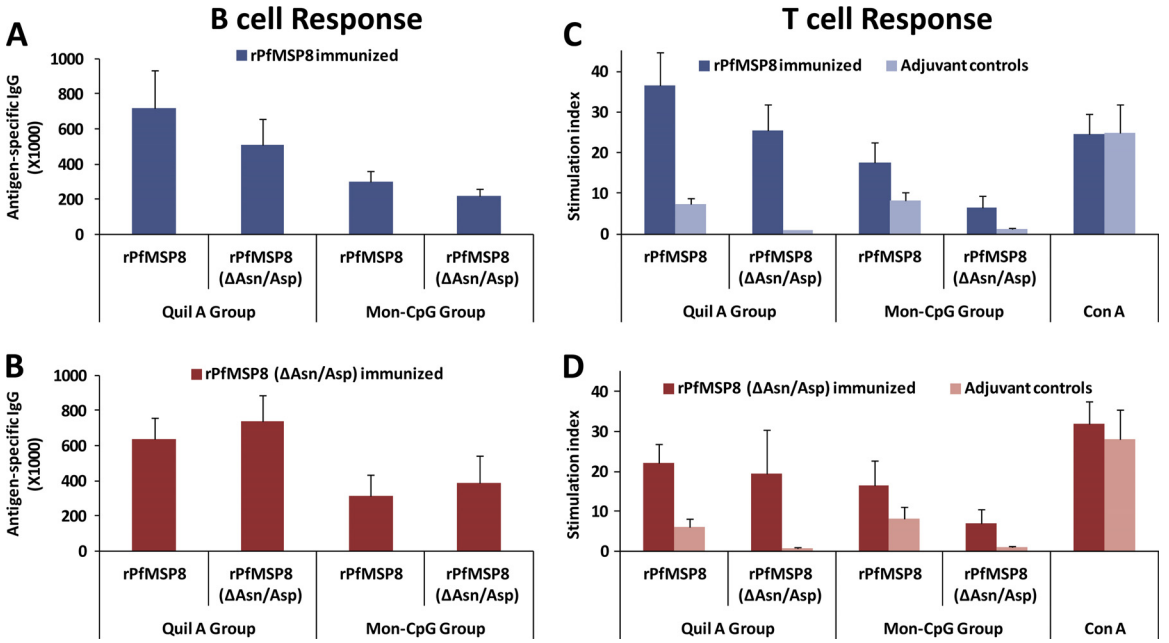

FIG 3 r*Pf*MSP8 and r*Pf*MSP8(ΔAsn/Asp) are immunogenic for both B cells and T cells in mice. Antigen-specific IgG titers in sera collected from CB6F1/J mice (5 mice/group) immunized with r*Pf*MSP8 (dark blue) (A) or r*Pf*MSP8(ΔAsn/Asp) (red) (B) formulated with Quil A or Montanide and CpG were determined by direct-binding ELISA on plates coated with either r*Pf*MSP8 or r*Pf*MSP8(ΔAsn/Asp) as indicated. For each dilution, the mean absorbance values at A_{405} of the pooled sera from adjuvant control mice ($n = 5$) was subtracted as the background. The *x* axis defines the adjuvant platform in each group. Splenocytes from mice immunized with r*Pf*MSP8 (dark blue) (C) or r*Pf*MSP8(ΔAsn/Asp) (red) (D) or adjuvant alone (light red or light blue) were stimulated with either r*Pf*MSP8 or r*Pf*MSP8(ΔAsn/Asp), and T cell proliferation was quantitated by measurement of [^{3}H]thymidine incorporation. The stimulation index was calculated as mean counts per minute in stimulated cultures/mean counts per minute in unstimulated cultures. Mean values ± standard deviations (SD) are shown. The *x* axis indicates the adjuvant used for immunization (Quil A or Montanide and CpG) and the specific stimulating antigen used in the proliferation assay.

4 out of 5 peptides located outside the C-terminal EGF-like domains. Peptides derived from the Asn/Asp-rich domain did not induce proliferative responses. As shown in Fig. 4B, this same set of five peptides induced significant and comparable proliferative responses of T cells from the r*Pf*MSP8(ΔAsn/Asp)-immunized mice. Similar results were obtained with splenocytes obtained from mice immunized with antigens formulated with Montanide and CpG (data not shown). Combined, these data indicate that the Asn/Asp-rich domain of *Pf*MSP8 is not immunogenic for T cells, and deletion of this domain in r*Pf*MSP8(ΔAsn/Asp) does not affect the magnitude or specificity of immunization-induced T cell responses.

Native *Pf*MSP8 undergoes proteolytic processing yielding a prominent, 17-kDa C-terminal membrane-anchored domain. To determine which domains of native *Pf*MSP8 are present and predominate, the ability of r*Pf*MSP8- and r*Pf*MSP8(ΔAsn/Asp)-specific antisera to recognize *Pf*MSP8 and/or its processed products in *P. falciparum* blood-stage parasites was evaluated. In immunoblot assays under nonreducing conditions, both rabbit anti-r*Pf*MSP8 and anti-r*Pf*MSP8(ΔAsn/Asp) antibodies detected three major bands of 80, 37, and 17 kDa (Fig. 5A) in extracts of asynchronous cultures of *P. falciparum* (FVO) blood-stage parasites. Under reducing conditions, the reactivity of the 37- and 17-kDa bands was abrogated, consistent with the presence of the C-terminal EGF-like domains of *Pf*MSP8 in these fragments. Unlike anti-r*Pf*MSP8(ΔAsn/Asp) antibodies, antibodies raised against r*Pf*MSP8 still detected the full-length 80-kDa protein under reducing conditions, likely due to the presence of antibodies specific for the Asn/Asp-rich domain (Fig. 5A). Notably, the three *Pf*MSP8-specific bands were similarly detected in four *P. falciparum* lines (FVO, 3D7, D10, and Dd2), attesting to the conserved nature of *Pf*MSP8 (Fig. 5B).

To further examine the kinetics of *Pf*MSP8 expression and processing through the asexual cycle, total antigen preparations from tightly synchronized *P. falciparum* blood-stage parasites were analyzed by immunoblot assay using rabbit anti-r*Pf*MSP8 IgG. As shown in Fig. 5C, the full-length 80-kDa *Pf*MSP8 was present through ring-stage development with peak levels in late ring/early trophozoite stages (20 h). As parasites differentiated further (26 to 40 h), the 80-kDa protein was lost, coinciding with the emergence of a weakly reactive 37-kDa band. The full-length 80-kDa *Pf*MSP8 could readily be detected again in very late-stage cultures (40- to 48-h time point). A prominent 17-kDa processed fragment persisted through the entire cycle, with peak levels in the latter half of the cycle (26 to 48 h). In free merozoites, the 80-kDa full-length *Pf*MSP8 was prominent along with low levels of the 17-kDa processed fragment and an additional immunoreactive band at 90 kDa, presumably nascent *Pf*MSP8 (Fig. 5C). Rabbit anti-r*Pf*MSP8 IgG failed to react with the EGF-like domains of $PfMSP1_{19}$, confirming specificity for *Pf*MSP8 (data not shown). Extracts from asynchronously growing parasites or free merozoites were subjected to two cycles of temperature-dependent Triton X-114 phase separation to generate a detergent phase (D) containing membrane-associated proteins and an aqueous phase (A) containing soluble proteins. As shown in Fig. 5D, the 17-kDa processed fragment of *Pf*MSP8 primarily partitioned in the detergent phase of both antigen preparations, consistent with the presence of a C-terminal GPI membrane anchor. Somewhat unexpectedly, the full-length 80-kDa *Pf*MSP8 partitioned primarily in the aqueous phase.

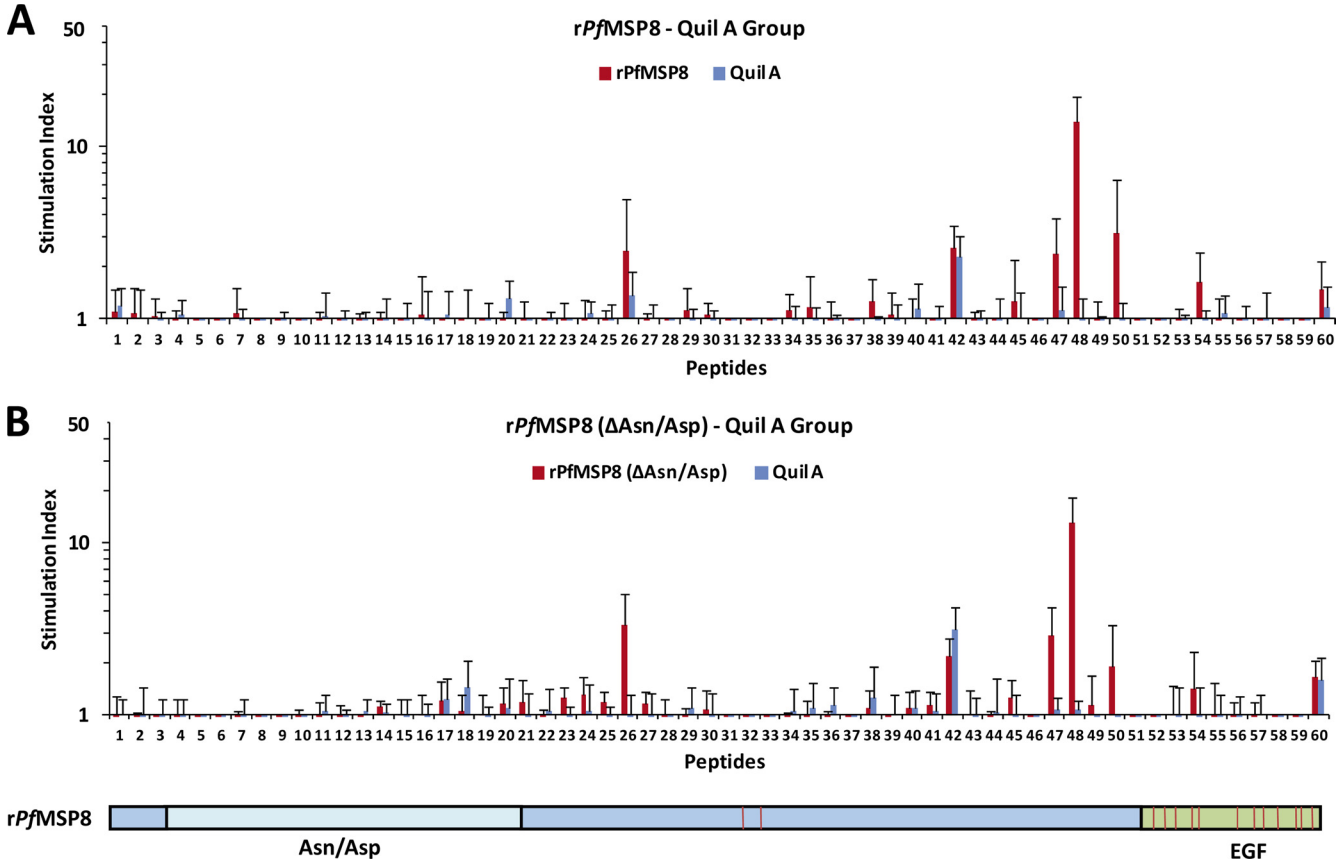

FIG 4 Deletion of the Asn/Asp-rich domain does not alter T cell epitope usage or immunogenicity of r*Pf*MSP8. Splenocytes from mice immunized with r*Pf*MSP8 (A) or r*Pf*MSP8(ΔAsn/Asp) (B) were stimulated with 15 μg/ml of overlapping synthetic peptides that spanned the entire length of the r*Pf*MSP8. T cell proliferation was quantitated as described above. Splenocytes from mice immunized with adjuvant alone were used as negative controls. Numbers on the *x* axis depict individual peptides (see Table S1 in the supplemental material) and are aligned with a schematic of recombinant *Pf*MSP8 at the bottom of the figure to show peptide positions within the coding sequence.

Native *Pf*MSP8 within free merozoites redistributes to the surface of ring-stage parasites. To determine if epitopes of native *Pf*MSP8 are accessible to serum antibodies, the localization of *Pf*MSP8 in *P. falciparum* blood-stage parasites was evaluated by immunofluorescence staining with rabbit anti-r*Pf*MSP8 and anti-r*Pf*MSP8(ΔAsn/Asp) IgG. *Pf*MSP8 expression was observed on the surface of ring- and trophozoite-stage parasites, with the peak staining in trophozoites (Fig. 6A). *Pf*MSP8 colocalized with *Pf*MSP1 only on the surface of early-ring-stage parasites. As the cycle progressed, *Pf*MSP1 levels declined as previously reported (19, 21). With the initiation of new synthesis later in the cycle, the characteristic staining of *Pf*MSP1 on the surface of individual merozoites in segmented schizonts was observed. In contrast, *Pf*MSP8-specific fluorescence in the segmented schizonts appeared rather punctuate, with discrete and pronounced staining within the parasite (Fig. 6A). *Pf*MSP8 was exclusively localized inside free merozoites in contrast to *Pf*MSP1, which was equally distributed on the parasite surface (Fig. 6B, top). Consistent with an internal and discrete localization in merozoites, *Pf*MSP8 also did not appear to colocalize with micronemal *Pf*AMA1 (Fig. 6B, bottom). Similar staining patterns were observed in immunofluorescence assays using rabbit anti-r*Pf*MSP8(ΔAsn/Asp) (data not shown).

Rabbit antibodies raised against r*Pf*MSP8 and r*Pf*MSP8 (ΔAsn/Asp) do not inhibit parasite growth *in vitro*. The ability of rabbit anti-r*Pf*MSP8 and anti-r*Pf*MSP8(ΔAsn/Asp) IgG to inhibit the *in vitro* growth of *P. falciparum* blood-stage parasites was measured. Neither rabbit anti-r*Pf*MSP8 nor rabbit anti-r*Pf*MSP8(ΔAsn/Asp) IgG significantly inhibited parasite growth compared to that of the adjuvant control IgG as determined by growth inhibition assays based on the measurement of parasite lactate dehydrogenase activity (Table 1) or [^{3}H]hypoxanthine incorporation (Table 2). Combined, these data indicate that *Pf*MSP8 is not a significant target of *in vitro* growth inhibitory antibodies, likely due to the low and/or transient expression of *Pf*MSP8 on the surface of extracellular merozoites.

DISCUSSION

Based on our earlier studies in the *P. yoelii* model, we became very interested in *Pf*MSP8 as a vaccine candidate and as a potential fusion partner for MSP1$_{19}$. In published studies, selected domains of *P. falciparum* MSP8 fused to GST and produced in recombinant form have been used for the production of polyclonal antisera for studies of the native antigen (5, 21). These GST fusion proteins have not been as useful for immunogenicity studies, where conformation of the full-length antigen may be important for antibody responses. Immunogenicity studies are further complicated by T cell recognition of GST epitopes. We attempted to produce nonfused, full-length r*Pf*MSP8 based on the native gene sequence

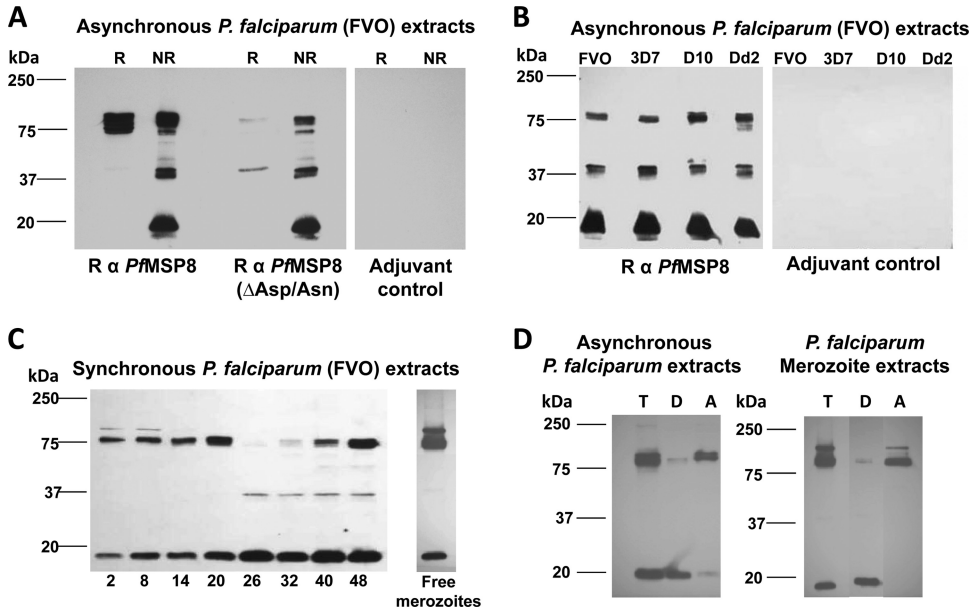

FIG 5 Native *Pf*MSP8 undergoes proteolytic processing yielding a 17-kDa, C-terminal membrane-anchored product. (A) Lysates of asynchronous *P. falciparum* (FVO) parasites were separated by SDS-PAGE under reducing (R) and nonreducing (NR) conditions and subjected to immunoblot analysis using rabbit anti-r*Pf*MSP8 or anti-r*Pf*MSP8(ΔAsn/Asp) IgG, with IgG obtained from rabbits immunized with adjuvant alone serving as a negative control. (B) Lysates of asynchronous *P. falciparum* 3D7, D10, and Dd2 parasites were subjected to immunoblot analysis under nonreducing conditions and probed with rabbit anti-r*Pf*MSP8 IgG or adjuvant control IgG. (C) Lysates of equal numbers of stage-separated, synchronous, *P. falciparum* (FVO) parasites were subjected to immunoblot analysis under nonreducing conditions and probed with rabbit anti-r*Pf*MSP8 IgG. (D) Asynchronous parasite or free merozoite pellets were lysed in the presence of ice-cold Triton X-114 and sampled for total antigen (T) before being subjected to temperature-dependent phase separation. The resulting detergent and aqueous phases were subjected to a second cycle of phase separation to yield the final detergent phase (D) and Triton X-114 depleted aqueous phase (A). Following SDS-PAGE under nonreducing conditions, aliquots of each sample were subjected to immunoblot analysis with rabbit anti-*Pf*MSP8 IgG. All IgGs (A to D) were used at a final concentration of 1 μg/ml. In each panel, molecular weight markers in kilodaltons (kDa) are indicated.

but were unsuccessful. We overcame this obstacle by applying the codon harmonization approach previously used in the production of *Pf*MSP1$_{42}$ and *Pf*LSA1 vaccines. We were very satisfied with both the quality and quantity of full-length r*Pf*MSP8 and truncated r*Pf*MSP8(ΔAsn/Asp). Purification proceeded under nondenaturing conditions with no need for refolding/renaturation. Success here enabled us to proceed with the evaluation of the immunogenicity and vaccine potential of *Pf*MSP8.

One clearly unique feature of *Pf*MSP8 relative to its orthologues in other plasmodial species is the presence of the ~170-amino-acid Asn/Asp-rich domain near the N terminus. *Pf*MSP8 polymorphism among the different *P. falciparum* strains is confined to this Asn/Asp-rich domain (5). Repeat sequences and/or regions of low complexity are common among *P. falciparum* proteins, some of which are implicated in important protein-protein interactions (37, 54). For vaccine considerations, repeat domains may provide potential targets of protective immunity as exemplified by the immunodominant protective B cell epitopes of the circumsporozoite protein (40). Undesirably, some repetitive epitopes have been postulated to function as decoys that redirect the immune responses away from functionally important domains (2, 15). Of interest, an N-terminal domain of *Pf*MSP8 that includes an Asn/Asp-rich sequence was shown to be recognized by natural antibodies in sera from individuals living in areas where malaria is endemic (5, 21). Initially, we focused on determining if this Asn/Asp-rich domain of *Pf*MSP8 was immunogenic for T and B cells and/or was important for the overall antigen conformation.

We compared the immunogenicity of full-length r*Pf*MSP8 and r*Pf*MSP8(ΔAsn/Asp). Both r*Pf*MSP8 and r*Pf*MSP8(ΔAsn/Asp) induced strong and equivalent antibody responses in mice and rabbits. Remarkably, the antibodies were highly cross-reactive, suggesting that the majority of the antibodies were directed toward determinants common to both recombinant proteins. Through a series of competitive binding ELISAs, we showed that (i) the conformations of domains common to the full-length r*Pf*MSP8 and the r*Pf*MSP8(ΔAsn/Asp) were similar, (ii) the majority of the antibodies elicited by immunization with full-length r*Pf*MSP8 or r*Pf*MSP8(ΔAsn/Asp) recognized disulfide-dependent epitopes, and (iii) a small, but detectable, fraction of antibodies induced by immunization with the full-length r*Pf*MSP8 recognized epitopes within the Asn/Asp-rich domain. We did note that the IC_{50}s for r*Pf*MSP8 as an inhibitor were consistently ~3-fold higher than for r*Pf*MSP8(ΔAsn/Asp) in parallel assays. These data suggest that the presence of the low-complexity, charged Asn/Asp-rich domain may influence, to some degree, binding of *Pf*MSP8-specific antibodies to proximal B cell epitopes. Both r*Pf*MSP8 and r*Pf*MSP8(ΔAsn/Asp) were equally immunogenic for T cells. Of interest, no T cell epitopes mapped to the Asn/Asp-rich domain, and removal of this domain did not alter T cell epitope usage in the remaining sequence. These data show that r*Pf*MSP8 is highly immunogenic for both B cells and T cells and that while the Asn/Asp-rich domain contributes modestly to the overall antibody response, its removal does not significantly alter antigen conformation and/or immunogenicity. Thus, r*Pf*MSP8(ΔAsn/Asp) appears to contain the dominant B and T cell epitopes of *Pf*MSP8.

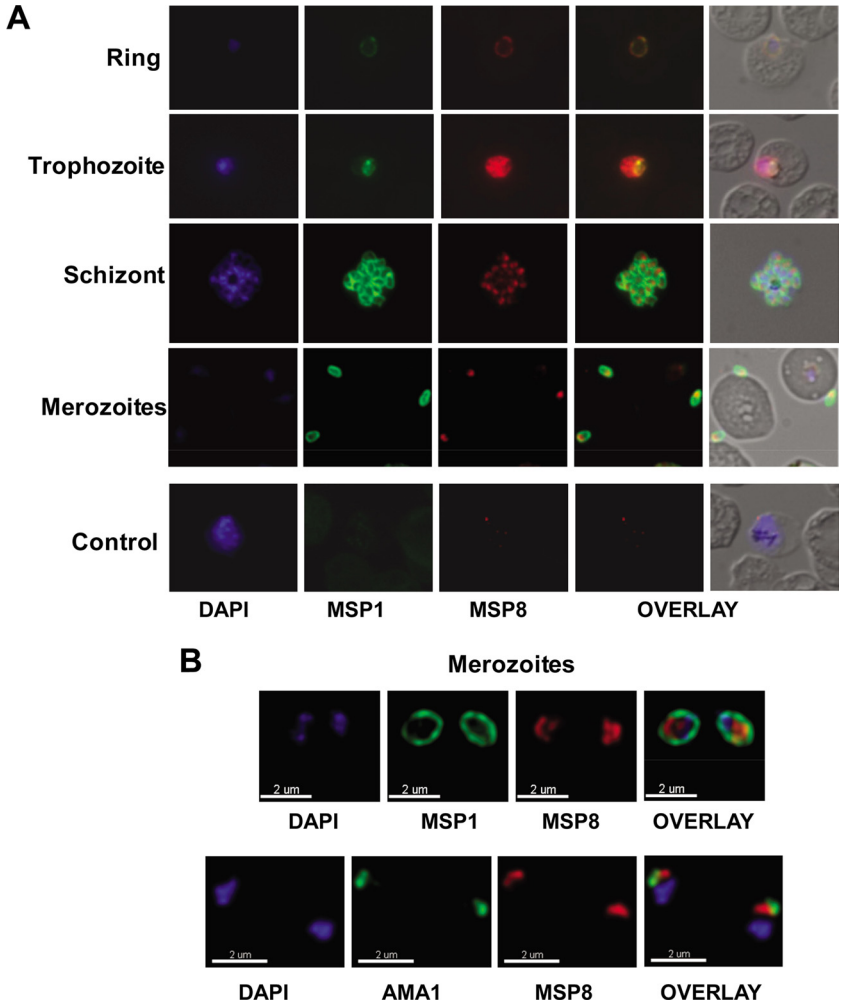

FIG 6 (A) Localization of *Pf*MSP8 in blood stages of the parasite. *Pf*MSP8 localization was evaluated by IFA using acetone-methanol-fixed slides of asynchronous *P. falciparum* (FVO)-infected erythrocytes. The smears were costained with rabbit anti-r*Pf*MSP8 IgG and mouse anti-*Pf*MSP1$_{19}$ (FVO) monoclonal antibody 5.2. Bound IgGs were detected by TRITC-conjugated goat anti-rabbit IgG and FITC-conjugated goat anti-mouse IgG and parasite DNA stained with DAPI. Shown are representative images of parasite DNA-specific fluorescence (blue) (column 1), *Pf*MSP1-specific fluorescence (green) (column 2), and *Pf*MSP8-specific fluorescence (red) (column 3), merged images of *Pf*MSP1 and *Pf*MSP8 (column 4), and merged images of DAPI, *Pf*MSP1, *Pf*MSP8, and the corresponding DIC images (column 5). Representative images of ring-, trophozoite-, schizont-, and merozoite-stage parasites are shown. "Control" represents corresponding images of infected RBCs stained with normal mouse sera and adjuvant control rabbit IgG. (B) Merozoite-associated *Pf*MSP8. In free merozoites, colocalization of *Pf*MSP8 with either *Pf*MSP1 (top) or *Pf*AMA1 (bottom) was evaluated by IFA as described above using rabbit anti-r*Pf*MSP8 IgG, MAb 5.2 (mouse anti-*Pf*MSP1$_{19}$ FVO), and MAb 4G2 (rat anti-*Pf*AMA1 FVO) with images acquired by confocal microscopy.

TABLE 1 *P. falciparum* GIA: lactate dehydrogenase levels[a]

IgG sample	IgG concn (mg/ml)	% inhibition
R α r*Pf*MSP8	5.0	1
	2.5	1
R α r*Pf*MSP8(ΔAsn/Asp)	5.0	−2
	2.5	0
Adjuvant control	5.0	3
	2.5	3
Control R α r*Pf*AMA1-C2	0.13	40
	0.78	84

[a] *In vitro* growth inhibitory activity of rabbit anti-*Pf*MSP8 IgG for *P. falciparum* FVO blood-stage parasites based on measurement of parasite lactate dehydrogenase levels. R α, rabbit anti-.

With the availability of full-length r*Pf*MSP8, we were able to produce high-titer, high-quality rabbit antisera for use in characterizing native, parasite-associated *Pf*MSP8. We were particularly interested in assessing similarities and differences between *P. fal-*

TABLE 2 *P. falciparum* GIA: [^{3}H]hypoxanthine incorporation[a]

IgG sample	IgG concn (mg/ml)	% inhibition
R α r*Pf*MSP8	1.0	−2
	0.5	0
R α r*Pf*MSP8(ΔAsn/Asp)	1.0	1
	0.5	2
Adjuvant control	1.0	0
	0.5	0

[a] *In vitro* growth inhibitory activity of rabbit anti-*Pf*MSP8 IgG for *P. falciparum* FVO blood-stage parasites based on parasite incorporation of [^{3}H]hypoxanthine. R α, rabbit anti-.

ciparum and *P. yoelii* MSP8, given the success of our vaccine studies in the rodent model. On immunoblots of *P. falciparum* blood-stage antigen lysates probed with rabbit anti-r*Pf*MSP8 and anti-r*Pf*MSP8(ΔAsn/Asp) antibodies, we detected 3 distinct bands of 80, 37, and 17 kDa. The sensitivity of the 37- and 17-kDa fragments to reduction suggest that the two fragments are likely C-terminally processed products of *Pf*MSP8 that include the EGF-like domains. While these results are in most part consistent with previous observations, Drew and colleagues (21) failed to detect the 37-kDa fragment. This could be explained by the transient nature of this fragment and/or the inherent differences in the specificities of the antibodies used. In our studies, the expression of the full-length *Pf*MSP8 appears to commence in late schizonts or early merozoites, with peak levels in late ring/early trophozoites. The initiation of *Pf*MSP8 expression we observed is earlier than previously suggested (21) but consistent with the profile for *Pf*MSP8 noted in microarray studies of global gene expression (9). Notably, both the 80- and 17-kDa fragments are present in lysates of free merozoites, suggesting that cleavage of the full-length *Pf*MSP8 to yield the 17-kDa fragment is rapid. In considering these results, it is important to note that we could not detect any cross-reactivity between the EGF-like domains of *Pf*MSP8 and *Pf*MSP1. This is consistent with previous reports demonstrating a lack of cross-reactivity between *Pf*MSP8 and other EGF-containing merozoite proteins, including MSP1, MSP4, and MSP5 (5), and the lack of reactivity of antibodies specific for *Pf*MSP8 with any blood-stage malarial proteins in *Pf*MSP8 knockout parasites (21).

The 17-kDa fragment of *Pf*MSP8 fractionated in a Triton X-114 detergent phase consistent with the presence of the predicted GPI anchor and appears to be the predominant processed product that persists through the asexual cycle as noted previously. We did not detect any significant amount of the 80-kDa *Pf*MSP8 in the Triton X-114 detergent phase as expected for a GPI-anchored protein. This suggested two possibilities. First, the addition of the GPI anchor to *Pf*MSP8 occurred at or near the time of proteolytic processing that yielded the 17-kDa, GPI-anchored C-terminal fragment of *Pf*MSP8. As noted above, proteolytic processing of *Pf*MSP8 appears to occur quickly after synthesis. Alternatively, the full-length *Pf*MSP8 possesses a GPI anchor, but the presence of the highly charged Asn/Asp-rich domain may affect its partitioning during Triton X-114 phase separation. At present, we cannot distinguish between these two possibilities. We have shown that *P. yoelii* MSP8 is GPI anchored with a similar pattern of expression, peaking in trophozoites (47). In marked contrast to *Pf*MSP8, proteolytic processing of *Py*MSP8 appears to be minimal, and it is the full-length protein that predominates through blood-stage development (47). In addition, we have demonstrated that full-length *Py*MSP8, which lacks the Asn/Asp-rich domain, possesses a GPI anchor as it fractionates with the detergent phase of Triton X-114-solubilized proteins and can be metabolically labeled with ^{3}H-palmitic acid (10).

Consistent with previous reports (5, 21), our immunofluorescence assays indicated that *Pf*MSP8 colocalizes with *Pf*MSP1 on the surface of early-ring-stage parasites and appears to be uniformly distributed on the surface of trophozoites. This is also consistent with our earlier studies examining the localization of MSP8 in *P. yoelii* in these stages. In our analysis, *Pf*MPS8 did not appear to concentrate within the food vacuole as Drew and colleagues observed (21). As schizonts developed, however, *Pf*MSP8-specific fluorescence progressively diminished until the very late stages, when newly synthesized *Pf*MSP8 appeared discretely packaged inside merozoites. In free merozoites, *Pf*MSP8 is exclusively localized intracellularly, while *Pf*MSP1 is uniformly distributed on the surface. As with the proteolytic processing data noted above, this differs to some degree relative to *P. yoelii* MSP8. As we reported previously, *Py*MSP8-specific fluorescence decreased as schizonts segmented, but at least a proportion of *Py*MSP8 remained on the merozoite surface and colocalized with *Py*MSP1 (47). Considering the localization of *Pf*MSP8 in merozoites and on ring-stage parasites, it is possible that *Pf*MSP8 redistributes to the parasite surface just before or after invasion of RBCs and, as suggested by Drew et al. (21), may be important in the formation and/or function of the parasitophorous vacuole. Combined, these data suggested that the function(s) of MSP8 in *P. falciparum* and *P. yoelii* overlap but may not be identical and that differences in MSP8 processing and/or localization may be related to the presence of the unique Asn/Asp-rich domain in *Pf*MSP8.

Immunization with *Py*MSP8 protects against lethal *P. yoelii* 17XL challenge, and this protection is dependent on antibodies that recognize conformation-dependent epitopes (10, 48). At this point, we cannot say how *Py*MSP8-specific antibodies provide protection *in vivo* and whether or not they inhibit merozoite invasion or postinvasion growth of intraerythrocytic parasites. Both possibilities have been suggested for MSP1-specific antibodies. With *P. falciparum*, neither our rabbit anti-r*Pf*MSP8 nor our rabbit anti-r*Pf*MSP8(ΔAsn/Asp) antibodies were able to inhibit the growth of blood-stage parasites *in vitro*. This may not be surprising considering, at best, a low and/or transient level of *Pf*MSP8 expression on the surface of free merozoites. However, it is also recognized that this *in vitro* assay of blood-stage parasite growth inhibition may not adequately reflect the complexity of the *in vivo* environment. Some antigen-specific antibodies may exert an antiparasite effect only when working cooperatively with other immune components. It may be possible to obtain *in vivo* data by r*Pf*MSP8 immunization of *Aotus* monkeys followed by *P. falciparum* challenge.

In the *P. yoelii* model, we showed that immunization with a chimeric antigen containing *Py*MSP1$_{19}$ fused to full-length *Py*MSP8 markedly improved protection against challenge infection compared to that of an admixture of *Py*MSP1$_{42}$ and *Py*MSP8 (49). Enhanced efficacy in part was due to the effects of *Py*MSP8-specific antibodies. However, a key to success of this vaccine was the improvement in the induction of antibodies specific for *Py*MSP1$_{19}$. Of significance, we showed that the MSP8-restricted T cell response was sufficient to provide help for both *Py*MSP1$_{19}$- and *Py*MSP8-specific B cells to produce high and sustained levels of protective antibodies (1, 49). Such a chimeric vaccine design may overcome some of the potential problems limiting the further development and testing of *Pf*MSP1$_{42}$-based vaccines. The MSP1$_{33}$ portion of *Pf*MSP1$_{42}$ does provide parasite-specific CD4 T cell epitopes (22, 32). However, there is some polymorphism associated with MSP1$_{33}$, and considering the clinical trial data (42), the strength of these MSP1$_{33}$-associated CD4 T cell epitopes may not be adequate for maximizing antibody responses to the protective MSP1$_{19}$. Furthermore, it also appears that the recognition of certain T cell epitopes within MSP1$_{33}$ may promote the development of antibodies which interfere with otherwise protective MSP1$_{19}$-specific antibodies (i.e., blocking antibodies) (46).

Given our previous *in vivo* data on *Py*MSP8 and the data pre-

sented here on *Pf*MSP8, we believe that use of *Pf*MSP8(ΔAsn/Asp) as a fusion partner for $PfMSP1_{19}$ to improve vaccine efficacy has promise. Deletion of the Asn/Asp region does not affect T cell or B cell immunogenicity. The *Pf*MSP8(ΔAsn/Asp) is highly conserved among *P. falciparum* isolates and contains potent $CD4^+$ T cell epitopes. Immunogenicity studies with a chimeric *Pf*MSP1/8 vaccine in comparison to $PfMSP1_{42}$ and *Pf*MSP8 will be informative in establishing the ability of *Pf*MSP8-specific T cells to provide help to $PfMSP1_{19}$-specific B cells. Any enhancement in the functional activity of $PfMSP1_{19}$-specific antibodies induced by *Pf*MSP1/8 can be measured using the *in vitro* growth inhibition assay. Positive results here would establish the basis for *in vivo* testing in nonhuman primates where the vaccine potential of *Pf*MSP8(ΔAsn/Asp) alone and a chimeric *Pf*MSP1/8 vaccine could be more fully evaluated.

ACKNOWLEDGMENTS

This work was supported by NIH-NIAID grant AI035661 (J.M.B.) and the Intramural Program of NIH-NIAID (C.A.L.).

We thank Kazutoyo Miura (NIH-NIAID) for providing the GIA data through the GIA Reference Center that is supported by the PATH Malaria Vaccine Initiative. We thank Prakash Srinivasan (NIH-NIAID) for assistance with the immunofluorescence analysis.

J.M.B. is an inventor listed on U.S. patent no. 7931908, entitled "Chimeric MSP-based malaria vaccine."

REFERENCES

1. **Alaro Jr, Lynch MM, Burns JM, Jr.** 2010. Protective immune responses elicited by immunization with a chimeric blood-stage malaria vaccine persist but are not boosted by *Plasmodium yoelii* challenge infection. Vaccine **28**:6876–6884.
2. **Anders RF, Coppel RL, Brown GV, Kemp DJ.** 1988. Antigens with repeated amino acid sequences from the asexual blood stages of *Plasmodium falciparum*. Prog. Allergy **41**:148–172.
3. **Angov E, et al.** 2003. Development and preclinical analysis of a *Plasmodium falciparum* merozoite surface protein-1(42) malaria vaccine. Mol. Biochem. Parasitol. **128**:195–204.
4. **Angov E, Hillier CJ, Kincaid RL, Lyon JA.** 2008. Heterologous protein expression is enhanced by harmonizing the codon usage frequencies of the target gene with those of the expression host. PLoS One **3**:e2189. doi:10.1371/journal.pone.0002189.
5. **Black CG, Wu T, Wang L, Hibbs AR, Coppel RL.** 2001. Merozoite surface protein 8 of *Plasmodium falciparum* contains two epidermal growth factor-like domains. Mol. Biochem. Parasitol. **114**:217–226.
6. **Black CG, Wu T, Wang L, Topolska AE, Coppel RL.** 2005. MSP8 is a nonessential merozoite surface protein in *Plasmodium falciparum*. Mol. Biochem. Parasitol. **144**:27–35.
7. **Blackman MJ, Heidrich HG, Donachie S, McBride JS, Holder AA.** 1990. A single fragment of a malaria merozoite surface protein remains on the parasite during red cell invasion and is the target of invasion-inhibiting antibodies. J. Exp. Med. **172**:379–382.
8. **Boyle MJ, et al.** 2010. Isolation of viable *Plasmodium falciparum* merozoites to define erythrocyte invasion events and advance vaccine and drug development. Proc. Natl. Acad. Sci. U. S. A. **107**:14378–14383.
9. **Bozdech Z, et al.** 2003. The transcriptome of the intraerythrocytic developmental cycle of *Plasmodium falciparum*. PLoS Biol. **1**:e5. doi:10.1371/journal.pbio.0000005.
10. **Burns JM, Jr, Belk CC, Dunn PD.** 2000. A protective glycosylphosphatidylinositol-anchored membrane protein of *Plasmodium yoelii* trophozoites and merozoites contains two epidermal growth factor-like domains. Infect. Immun. **68**:6189–6195.
11. **Burns JM, Jr, et al.** 1989. A protective monoclonal antibody recognizes a variant-specific epitope in the precursor of the major merozoite surface antigen of the rodent malarial parasite *Plasmodium yoelii*. J. Immunol. **142**:2835–2840.
12. **Chappel JA, Holder AA.** 1993. Monoclonal antibodies that inhibit *Plasmodium falciparum* invasion in vitro recognise the first growth factor-like domain of merozoite surface protein-1. Mol. Biochem. Parasitol. **60**:303–311.
13. **Chowdhury DR, Angov E, Kariuki T, Kumar N.** 2009. A potent malaria transmission blocking vaccine based on codon harmonized full length Pfs48/45 expressed in *Escherichia coli*. PLoS One **4**:e6352. doi:10.1371/journal.pone.0006352.
14. **Collins CR, et al.** 2007. Fine mapping of an epitope recognized by an invasion-inhibitory monoclonal antibody on the malaria vaccine candidate apical membrane antigen 1. J. Biol. Chem. **282**:7431–7441.
15. **Cowman AF, et al.** 1985. Conserved sequences flank variable tandem repeats in two S-antigen genes of *Plasmodium falciparum*. Cell **40**:775–783.
16. **Daly TM, Long CA.** 1995. Humoral response to a carboxyl-terminal region of the merozoite surface protein-1 plays a predominant role in controlling blood-stage infection in rodent malaria. J. Immunol. **155**:236–243.
17. **de Marco A.** 2009. Strategies for successful recombinant expression of disulfide bond-dependent proteins in *Escherichia coli*. Microb. Cell Fact. **8**:26.
18. **Desjardins RE, Canfield CJ, Haynes JD, Chulay JD.** 1979. Quantitative assessment of antimalarial activity in vitro by a semiautomated microdilution technique. Antimicrob. Agents Chemother. **16**:710–718.
19. **Dluzewski AR, et al.** 2008. Formation of the food vacuole in *Plasmodium falciparum*: a potential role for the 19 kDa fragment of merozoite surface protein 1 (MSP1(19)). PLoS One **3**:e3085. doi:10.1371/journal.pone.0003085.
20. **Drew DR, O'Donnell RA, Smith BJ, Crabb BS.** 2004. A common cross-species function for the double epidermal growth factor-like modules of the highly divergent plasmodium surface proteins MSP-1 and MSP-8. J. Biol. Chem. **279**:20147–20153.
21. **Drew DR, Sanders PR, Crabb BS.** 2005. *Plasmodium falciparum* merozoite surface protein 8 is a ring-stage membrane protein that localizes to the parasitophorous vacuole of infected erythrocytes. Infect. Immun. **73**:3912–3922.
22. **Egan A, Waterfall M, Pinder M, Holder A, Riley E.** 1997. Characterization of human T- and B-cell epitopes in the C terminus of *Plasmodium falciparum* merozoite surface protein 1: evidence for poor T-cell recognition of polypeptides with numerous disulfide bonds. Infect. Immun. **65**:3024–3031.
23. **Egan AF, et al.** 1996. Clinical immunity to *Plasmodium falciparum* malaria is associated with serum antibodies to the 19-kDa C-terminal fragment of the merozoite surface antigen, PfMSP-1. J. Infect. Dis. **173**:765–769.
24. **Feachem RG, et al.** 2010. Shrinking the malaria map: progress and prospects. Lancet **376**:1566–1578.
25. **Hackett F, Sajid M, Withers-Martinez C, Grainger M, Blackman MJ.** 1999. PfSUB-2: a second subtilisin-like protein in *Plasmodium falciparum* merozoites. Mol. Biochem. Parasitol. **103**:183–195.
26. **Harris PK, et al.** 2005. Molecular identification of a malaria merozoite surface sheddase. PLoS Pathog. **1**:241–251. doi:10.1371/journal.ppat.0010029.
27. **Hensmann M, et al.** 2004. Disulfide bonds in merozoite surface protein 1 of the malaria parasite impede efficient antigen processing and affect the in vivo antibody response. Eur. J. Immunol. **34**:639–648.
28. **Hillier CJ, et al.** 2005. Process development and analysis of liver-stage antigen 1, a preerythrocyte-stage protein-based vaccine for *Plasmodium falciparum*. Infect. Immun. **73**:2109–2115.
29. **Hirunpetcharat C, et al.** 1997. Complete protective immunity induced in mice by immunization with the 19-kilodalton carboxyl-terminal fragment of the merozoite surface protein-1 (MSP1[19]) of *Plasmodium yoelii* expressed in *Saccharomyces cerevisiae*: correlation of protection with antigen-specific antibody titer, but not with effector CD4+ T cells. J. Immunol. **159**:3400–3411.
30. **Holder AA.** 2009. The carboxy-terminus of merozoite surface protein 1: structure, specific antibodies and immunity to malaria. Parasitology **136**:1445–1456.
31. **Holder AA, Freeman RR.** 1984. The three major antigens on the surface of *Plasmodium falciparum* merozoites are derived from a single high molecular weight precursor. J. Exp. Med. **160**:624–629.
32. **Huaman MC, et al.** 2008. Ex vivo cytokine and memory T cell responses to the 42-kDa fragment of *Plasmodium falciparum* merozoite surface protein-1 in vaccinated volunteers. J. Immunol. **180**:1451–1461.
33. **Kumar S, et al.** 1995. Immunogenicity and in vivo efficacy of recombi-

nant *Plasmodium falciparum* merozoite surface protein-1 in *Aotus* monkeys. Mol. Med. **1**:325–332.
34. **Li X, et al.** 2004. A coligand complex anchors *Plasmodium falciparum* merozoites to the erythrocyte invasion receptor band 3. J. Biol. Chem. **279**:5765–5771.
35. **Ling IT, Ogun SA, Holder AA.** 1994. Immunization against malaria with a recombinant protein. Parasite Immunol. **16**:63–67.
36. **Lyon JA, Geller RH, Haynes JD, Chulay JD, Weber JL.** 1986. Epitope map and processing scheme for the 195,000-dalton surface glycoprotein of *Plasmodium falciparum* merozoites deduced from cloned overlapping segments of the gene. Proc. Natl. Acad. Sci. U. S. A. **83**:2989–2993.
37. **Magowan C, et al.** 2000. *Plasmodium falciparum* histidine-rich protein 1 associates with the band 3 binding domain of ankyrin in the infected red cell membrane. Biochim. Biophys. Acta **1502**:461–470.
38. **McBride JS, Heidrich HG.** 1987. Fragments of the polymorphic Mr 185,000 glycoprotein from the surface of isolated *Plasmodium falciparum* merozoites form an antigenic complex. Mol. Biochem. Parasitol. **23**:71–84.
39. **Miura K, et al.** 2008. Comparison of biological activity of human anti-apical membrane antigen-1 antibodies induced by natural infection and vaccination. J. Immunol. **181**:8776–8783.
40. **Nussenzweig V, Nussenzweig RS.** 1985. Circumsporozoite proteins of malaria parasites. Cell **42**:401–403.
41. **O'Donnell RA, et al.** 2001. Antibodies against merozoite surface protein (MSP)-1(19) are a major component of the invasion-inhibitory response in individuals immune to malaria. J. Exp. Med. **193**:1403–1412.
42. **Ogutu BR, et al.** 2009. Blood stage malaria vaccine eliciting high antigen-specific antibody concentrations confers no protection to young children in Western Kenya. PLoS One **4**:e4708. doi:10.1371/journal.pone.0004708.
43. **Pachebat JA, et al.** 2007. Extensive proteolytic processing of the malaria parasite merozoite surface protein 7 during biosynthesis and parasite release from erythrocytes. Mol. Biochem. Parasitol. **151**:59–69.
44. **Pachebat JA, et al.** 2001. The 22 kDa component of the protein complex on the surface of *Plasmodium falciparum* merozoites is derived from a larger precursor, merozoite surface protein 7. Mol. Biochem. Parasitol. **117**:83–89.
45. **Painter HJ, Morrisey JM, Mather MW, Vaidya AB.** 2007. Specific role of mitochondrial electron transport in blood-stage *Plasmodium falciparum*. Nature **446**:88–91.
46. **Pusic KM, et al.** 2011. T cell epitope regions of the *P. falciparum* MSP1-33 critically influence immune responses and in vitro efficacy of MSP1-42 vaccines. PLoS One **6**:e24782. doi:10.1371/journal.pone.0024782.
47. **Shi Q, Cernetich-Ott A, Lynch MM, Burns JM, Jr.** 2006. Expression, localization, and erythrocyte binding activity of *Plasmodium yoelii* merozoite surface protein-8. Mol. Biochem. Parasitol. **149**:231–241.
48. **Shi Q, et al.** 2005. Alteration in host cell tropism limits the efficacy of immunization with a surface protein of malaria merozoites. Infect. Immun. **73**:6363–6371.
49. **Shi Q, Lynch MM, Romero M, Burns JM, Jr.** 2007. Enhanced protection against malaria by a chimeric merozoite surface protein vaccine. Infect. Immun. **75**:1349–1358.
50. **Shi YP, et al.** 1996. Natural immune response to the C-terminal 19-kilodalton domain of *Plasmodium falciparum* merozoite surface protein 1. Infect. Immun. **64**:2716–2723.
51. **Smythe JA, et al.** 1988. Identification of two integral membrane proteins of Plasmodium falciparum. Proc. Natl. Acad. Sci. U. S. A. **85**:5195–5199.
52. **Thanaraj TA, Argos P.** 1996. Ribosome-mediated translational pause and protein domain organization. Protein Sci. **5**:1594–1612.
53. **Trucco C, et al.** 2001. The merozoite surface protein 6 gene codes for a 36 kDa protein associated with the *Plasmodium falciparum* merozoite surface protein-1 complex. Mol. Biochem. Parasitol. **112**:91–101.
54. **Waller KL, Cooke BM, Nunomura W, Mohandas N, Coppel RL.** 1999. Mapping the binding domains involved in the interaction between the *Plasmodium falciparum* knob-associated histidine-rich protein (KAHRP) and the cytoadherence ligand *P. falciparum* erythrocyte membrane protein 1 (PfEMP1). J. Biol. Chem. **274**:23808–23813.